Chapter 3
Fluid-Flow Characterization in Microfluidics

Laura Campo-Deaño

Abstract The number of scientific studies related with microfluidics techniques have been increasing in the last decade due to the great advantages they provide in the characterization of complex fluid flows. Obtaining precise and accurate results, especially in the experimental field, is of great importance. However, this is not always an easy task. In this chapter we analyze fundamental aspects related to the experimental techniques in microfluidics, providing also some useful tips to assist anyone who decides to start in this exciting "micro world". A brief introduction about the potentialities of microfluidics will be presented. Additionally, a small review of the most common experimental techniques and their advantages and disadvantages are also assessed. Finally, an overview of the most common errors/difficulties of these experimental techniques in the lab is introduced.

3.1 Introduction

As it was stated along this book, microfluidics is a powerful technology based on the manipulation of tiny volumes of fluid. This technique constitutes a new alternative to study and solve some fluid flow complex problems in which the conventional macro techniques are not able to reach. Particularly in the area of biomedicine, to provide new assays system for blood characterization, blood separation, drug delivery, but also as an useful tool when the available material to test, i.e. the amount of fluid, is very limited or costly.

As a first step to understand why the complex fluid flow at micro scale is so different from the complex fluid flow at macro scale, we will examine the most important dimensionless numbers that play a very important role. One of them is the Reynolds number, which is the relation between the inertial and viscous forces and can be expressed as $Re = (\rho VL)/\eta$, where η and ρ are the viscosity and the density of the fluid, respectively, V the average velocity and L the characteristic length of

L. Campo-Deaño (✉)
Department of Mechanical Engineering, Faculty of Engineering of the University of Porto, Rua Dr. Roberto Frias s/n, 4200-465 Porto, Portugal
e-mail: campo@fe.up.pt

F.J. Galindo-Rosales (ed.), *Complex Fluid-Flows in Microfluidics*,
DOI 10.1007/978-3-319-59593-1_3

the micro channel. Considering water as working fluid, velocities of the order of 1 μm/s or cm/s and typical length scales of 100 or 1 μm, the Reynolds number will vary between 10^{-6} and 1, and it is possible to affirm that viscous forces typically dominate over inertial forces. Therefore, the flow in micro devices can be considered laminar even when the working fluid presents very low viscosity [20, 27].

When dealing with complex fluids, another important parameter is the Weissemberg number, which account for the relation of the relaxation time of the fluid (λ) and the flow deformation time, $Wi = \lambda(V/L)$, being λ the relaxation time of the fluid. On the other hand, another similar dimensionless parameter is the Deborah number, defined as the relation between the relaxation time of the fluid and the time of observation of the flow (t), $De = \lambda/t$, that helps (as in the case of the Wi number) to characterize flows presenting some degree of elasticity apart, obviously, from viscosity. In microfluidics, the combination of the high deformation rates, small time scale and small characteristic length leads to attain high De or Wi numbers meanwhile the Re is relatively low. This fact favors the observation of strong viscoelastic effects that, in the case of very low viscoelastic fluids, would be hided by inertial effects at the macro scale [20].

Taking these considerations into account, it is easy to understand how the complex flows in micro scale are too different from the complex flows at macro scale.

In microfluidics, the micro channels can be either designed for mimicking an specific geometry to reproduce *in vitro* some natural or biological phenomena [5, 15, 17, 24], to study the flow dynamics around different bodies [4, 14] or specially designed to analyze the viscoelastic properties of complex fluids, i.e. rheometer-on-a-chip (Fig. 3.1).

In this latter case, several progress have been performed in the last years [2, 11, 19, 22, 33]. Pipe and McKinley [23] wrote an interesting review about the use of microfluidics techniques to measure rheological properties in shear and extensional flows. In a more recent review Galindo-Rosales et al. [10] present a nice overview of several micro channel designed to characterize the extensional properties of fluids. More information about microrheometry can be found in Chap. 1.

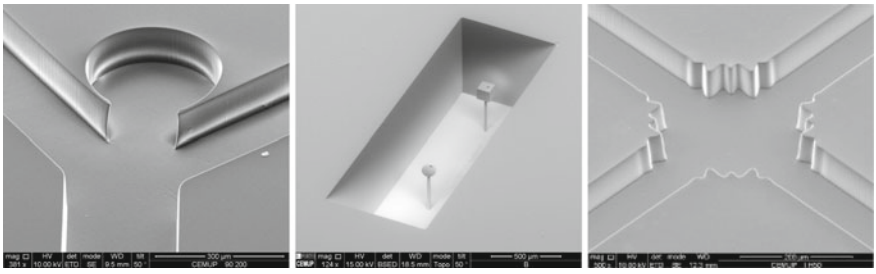

Fig. 3.1 Scanning Electron Microscopy (SEM) images for different geometry micro channels. *Left* simplified 2D micro channels mimicking an aneurysm; *centre* 3D microbot prototypes; *right* optimized cross-slot geometry for generating pure extensional flows

In order to characterize the main features of the complex flows in micro scale it is very common to use different experimental techniques. These techniques are able to provide the velocity profiles along the micro channels, the streamlines, pressure drop differences and even the stress distribution. A more detailed review of these experimental techniques will be presented in the following section.

The contents in this chapter book are as follows: after the Introduction, Sect. 3.2 will deal with the experimental techniques commonly used in microfluidics for the characterization of complex fluid-flows; in Sect. 3.3, some tips on how to solve possible experimental problems will be presented, and finally, some remarks are explained in Sect. 3.4.

3.2 Experimental Techniques

The working fluids used in microfluidics are normally transparent, making impossible to analyze the flow pattern as the fluid motion is invisible for us. In order to overcome this limitation, different methods can be considered, such as visualizing the surface flow (i.e. adding colored oil to the surface channel), analyzing the changes in the refractive index of the flow or by adding tracer particles to the flow. The latter one is the most common technique used in microfluidics and hereafter we will refer to this methodology. The nature and size of the tracer particles will depend on the characteristic of the fluid, the morphology of the micro channels and also on the intrinsic characteristic of the experimental technique. In general, the tracer particles must to present the following characteristics: their density should be close to the density of the working fluid; they have to be non-volatile, non-toxic or corrosive and they should not undergo any chemical reaction; and they should present an optimum size [7].

A proper design of the experimental set up and an accurate assembly of all its components is crucial for a precise analysis of the flow behavior in micro channels. The equipment of a complete set up varies according the experimental technique, however as a general rule a microfluidic setup for the study of the flow behavior of complex fluid flows must be composed of the following items:

- Inverted microscope equipped with a CCD camera, a light source and a filter cube.
- Syringe pump to inject the fluid and control the flow rate in the micro channel.
- Syringes with different volumes.
- Tubes for connecting the syringes with the channels.
- Connectors, valves and tips.
- Micro channel geometries.
- Working fluids.
- Computer.

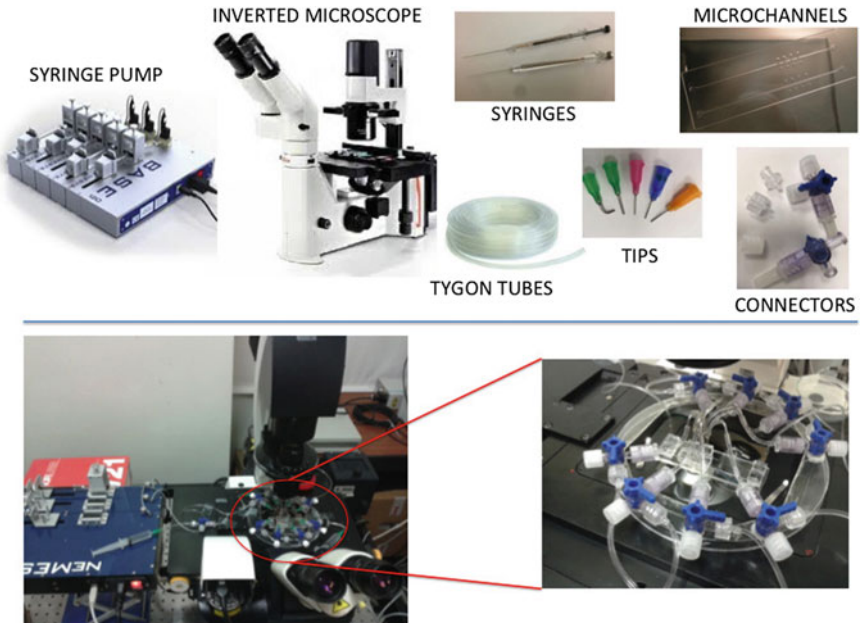

Fig. 3.2 General setup for a microfluidic experiment. The syringe pump image is courtesy from CETONI, GmbH. This modular pump offers an extremely precise and stable flow with virtually no pulsation. Image of the inverted microscope is courtesy from Leica Microsystems

A proper design of the microfluidic set up is crucial for obtaining reliable and accurate measurements of the main flow characteristics.

Example of a general microfluidic set up is shown in Fig. 3.2. The main components as the syringe pump, the microscope, syringes, supply tubes and micro channels are essential independently of the experimental technique.

More detail about the properties of each component of the setup will be covered in the following subsections for each particular technique. In Fig. 3.3 the most common flow characterization techniques are summarized according to their applicability. It is necessary to point out that these techniques are non-invasive and therefore its applicability does not interfere in the rheological properties of the fluid either in the fluid flow behavior.

Knowing the potentialities and applicability of the available experimental techniques is crucial for the selection of the most appropriate method for fluid flow characterization.

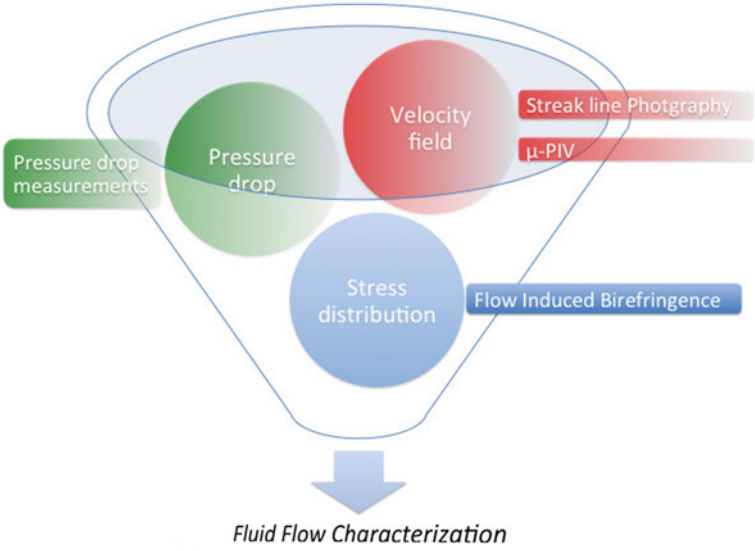

Fig. 3.3 Overview of the main experimental techniques for fluid flow characterization in microfluidics

3.2.1 Streak Line Photography

Streak line photography is a flow visualization technique that can be applied either at macro or at micro scale. It consists on recording particles displacements over a period of time, allowing a qualitative analysis of the flow pattern. The fluids should be seeded with fluorescent tracer particles, it is also recommendable to add an small amount of surfactant, i.e. Sodium Dodecyl Sulfate (SDS), around 0.05 wt%, to diminish adhesion of the tracer particles to the micro channel walls.

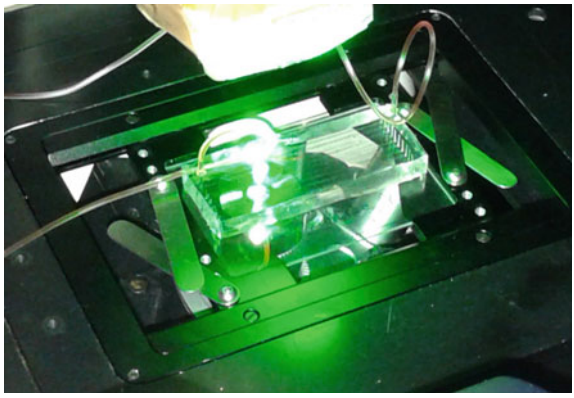

Fig. 3.4 Mercury lamp illumination during a streak line photography experiment

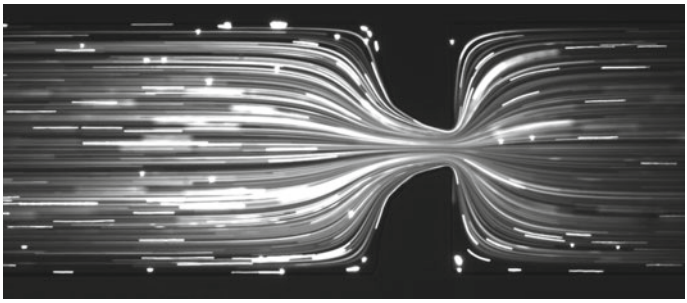

Fig. 3.5 Flow visualization using streak line photography technique of a viscoelastic fluid flowing through a contraction-expansion geometry

The micro channels which contain the seeded fluid is continuously illuminated using a mercury lamp (Fig. 3.4) and the light emitted by the tracers is imaged through the objective lens onto the CCD array of the camera using long exposure times to capture the pathlines of the particles. The exposure times should be varied accordingly with the flow rate and the dimensions of the channels. Figure 3.5 shows a viscoelastic fluid flow through a contraction-expansion geometry using streak line photography.

3.2.2 Micro—Particle Image Velocimetry (μ-PIV)

Particle image velocimetry is an imaging method normally used for quantifying the velocity field which results from the measure of the local velocity based on the average displacement of fluorescent particles in an interrogation area over a known time. The motion of these particles within each interrogation region is determined using cross correlation algorithms [30].

For its use in microfluidics, it is normally to perform a μ-PIV technique which presents some fundamental differences from the macro-PIV technique. In conventional PIV a light sheet is used to illuminate the tracer particles, while in μ-PIV a volume illumination is applied and interactions between particles and particles-fluid can originate Brownian motion due to their small size. The spatial resolution of this experimental technique depends on the tracer particle size, tracer particle density and image quality, among others [25]. In order to perform accurate micro-PIV measurements some considerations must be taking into account according to [18], mainly:

- *In-plane spatial resolution*: the tracer particles used in this technique should be imaged with enough high magnification, about three-four pixels in diameter. The diffraction limited spot size of a point source of light d_s is as follows:

$$d_s = 2.44(M+1)\frac{\lambda}{2NA} \tag{3.1}$$

where M is the magnification of the objective λ is the wavelength of the light emitted or scattered by the tracer particles and NA the numerical aperture of the lens. The effective image diameter can be expressed as:

$$d_e = [d_s^2 + M^2 d_p^2]^{1/2} \tag{3.2}$$

being d_p the real particle diameter. When Md_p is smaller than d_s the diffraction effects dominate and d_s remains constant. If the image size is larger than d_s, then $d_e \approx Md_p$.

- *Out-of-plane spatial resolution*: the measurement plane is normally determined using the depth of field of the objective lens used. As the flow field is volume-illuminated in micro-PIV techniques, particles that are out-of-focus should be considered as they are contributing for the background noise. So, the thickness of the measurement plane, δz_m, (Fig. 3.6) is obtained taking into account three different effects: one due to geometrical optics, another one due to the finite size of the particle and finally, the effect of the diffraction (Eq. 3.3) [26]

$$\delta z_m = \frac{3n\lambda_0}{(NA)^2} + \frac{2.16d_p}{tan\theta} + d_p \tag{3.3}$$

being n the refractive index, λ_0 is the wavelength of light, d_p the particle diameter and $tan\theta \approx sin\theta = NA/n$.
As it was stated above, due to the application of a volume illumination there are some unfocused particles that are contributing for the background noise. This noise is very difficult to remove as it normally presents the same wavelength as the focused particle. Then, the particle visibility, which is the ratio of the intensity of an in focus particle image to the background light produced by the out of focus particles, can be determined by the theory of Olsen and Adrian [21]. They found that particle visibility is increased by decreasing particle concentration or by decreasing the thickness of the test section. Also, the visibility would increase decreasing the particle diameter or increasing the NA of the lens, keeping constant the concentration of particles. They derived an equation for the volume fraction, V_{fr} of particles that produces a particular visibility (V):

$$V_{fr} = \frac{2d_p^3 M^2 \beta^2 (s_0 - L/2)(s_0 - L/2 + L)}{3VLs_0^2[M^2 d_p^2 + 1.49(M+1)^2\lambda^2[(n/NA)^2 - 1]} \tag{3.4}$$

where s_0 is the objective working distance and L the depth of the micro channel. β^2=3.67 defines the cut-off level of the edges of the particle. A visibility of about 1.5 is required for high quality velocity measurements.

- *Effects of Brownian motions*: the Brownian motion undergone by the tracer particles when they are very small can provoke errors in the velocity measurements and also can lead to a uncertainty in the location of the particles. As a consequence

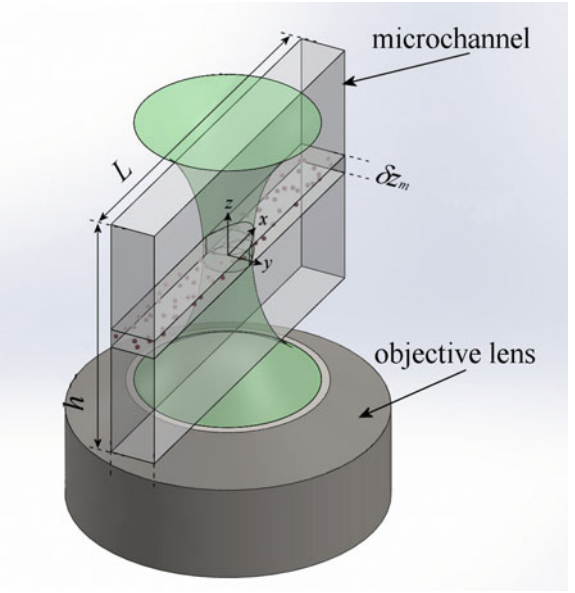

Fig. 3.6 Schematic representation of the volume illumination and the measurement plane, δz_m. Image courtesy of Simon J. Haward (OIST, Japan)

of imaging the Brownian particle displacements, the relative errors in x and y components of the velocity are:

$$\varepsilon_x = \frac{\sigma_x}{\Delta x} = \frac{1}{u}\sqrt{\frac{2D}{\Delta t}} \tag{3.5}$$

$$\varepsilon_y = \frac{\sigma_y}{\Delta y} = \frac{1}{u}\sqrt{\frac{2D}{\Delta t}} \tag{3.6}$$

where σ is the displacement of the particles in each direction, Δx and Δy are the total particle displacement, u and v are the velocity components in x and y directions, Δt is the time interval between images and D is the diffusion coefficient:

$$D = \frac{k_B T}{3\pi \mu d_p} \tag{3.7}$$

being k_B the Boltzmann's constant (k_B = 1.3807 × 10^{-23} m^2 kg/ s^2 K), T the absolute temperature and μ the dynamic viscosity of the fluid [28].
Therefore, it is possible to affirm that the effect of the Brownian motion of the particles is very low for faster flows.

3.2.3 Pressure Drop Measurements

This experimental technique provides valuable information in microfluidics. Different pressure sensors covering various differential pressure ranges can be employed according to the pressure drop one wanted to measure, which depends on the channel characteristics and the flow rates under study. The most common pressure sensors used in this area are capacitive or piezoresistive. In the last years, piezoresistive sensors systems with high preciseness and sensitivity for pressure measurements have been developed, and they are able to measure absolute and relative pressure (Fig. 3.7) [6, 8].

The differential pressure sensors, normally used in microfluidics, should be calibrated utilizing two different methods: a static column of water for sensors covering small pressure differences and a compressed air line with a manometer for sensors covering higher differential pressures. For that end, two pressure ports must be located upstream and downstream of the area of study. The pressure sensors are powered by a power supply and connected to a computer using a data acquisition card to register the data (voltage). Figure 3.8 shows a typical calibration curve for a differential pressure sensor, it is clear a linear dependence of the voltage with the imposed pressure difference in a water column ($\Delta P = \rho g \Delta h$).

The pressure sensors typically show a transient response until steady-state is reached. For Newtonian fluids, the steady-state is reached more rapidly than for viscoelastic fluids (Fig. 3.9). After steady-state is attained, the signal reaches a plateau with superimposed low amplitude oscillations due mostly to electronic noise, and the average pressure drop is calculated by taking the arithmetic mean of the signal with time [2].

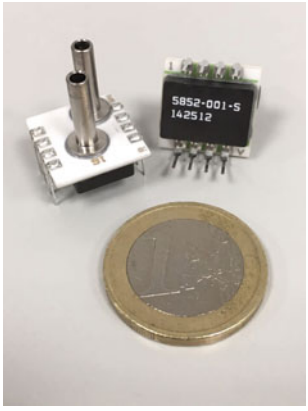

Fig. 3.7 Image of a differential pressure sensor used in microfluidics

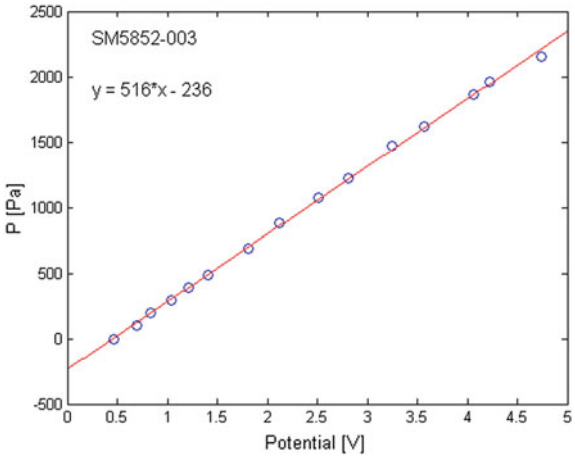

Fig. 3.8 Typical calibration *curve* for a differential pressure sensor

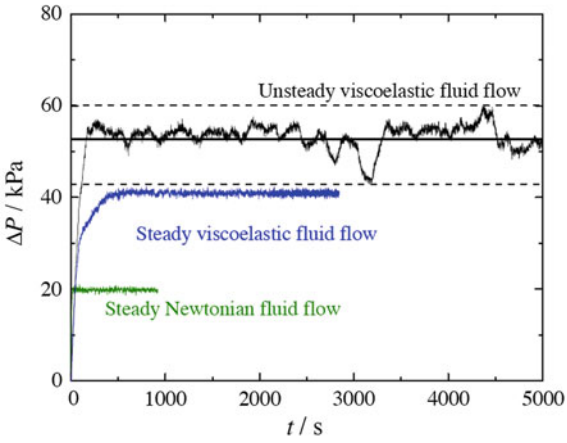

Fig. 3.9 Pressure drop measurements as a function of time for Newtonian and viscoelastic fluids. Image courtesy of Patrícia C. Sousa (FEUP, Portugal)

3.2.4 Birefringence Techniques

Flow induced birefringence (FIB) is a non-invasive technique for measuring the stress distribution in polymer solutions. FIB is caused by small changes in the refraction of light passing through a fluid flow, and these changes correlate to elastic stresses in the flowing fluid [12]. The level of birefringence is higher as the polymer chains are elongated which implies higher stresses [32].

The applicability of FIB techniques requires the use of birefringent materials introducing a restriction to the fluids being used.

For obtaining an optical birefringence pattern, the micro channels containing the working fluid are continuous illuminated using a monochromatic light. A helium-neon laser is normally used to allow the beam passed orthogonally through the micro channel. The laser is detected by a CCD camera recording at the area of interest. On each side of the micro channel, a polarizer and a analyser are located with axes at 45° to the flow axis, and at 90° to each other in order to diminish the signal taken by the camera. A λ/4 plate, which is a retardation plate causing a phase difference of $\pi/2$, is used to balance the residual birefringence in the micro channel and is placed within the polarizer and analyser. Around 20–25 ms images are normally captured at different flow rates. At the moment at which the flow is stopped, the background image is captured and removed from the images obtained under flow to show the birefringent signal. The intensity of the signal is calibrated by means of a λ/30 compensator in the optical line, when the compensator is rotated the intensity of the signal is obtained in order to get a range of retardation values. The relation between the retardation, R, and the birefringence, Δn, is as follows: $R = \Delta n\, l$, where l is the path-length through the material.

The normal stress and the shear stress can be obtained by means of the stress-optic law [16]. Equations 3.8 and 3.9 provides the relationship between the index of refraction tensor and the stress tensor:

$$\sigma_{12} = \frac{1}{2C}\Delta n sin(2\alpha), \tag{3.8}$$

$$\sigma_{11} - \sigma_{22} = \frac{1}{C}\Delta n cos(2\alpha), \tag{3.9}$$

being C the stress-optic coefficient which is independent of molecular weight, polydispersity, and polymer concentration [13, 29].

Birefringence measurements provide the stress tensor directly only when the flow is considered to be 2D. Otherwise, for a 3D flow, the birefringence and the orientation angle vary along the light path leading to a cumulative measurement of the optical properties [32].

3.3 Some Typical Errors/Difficulties

It is normal that before and during the experimentation different kind of difficulties appear. In this section, some of these problems are summarized as well as some tips in order to help to overcome these complications.

3.3.1 Optical Distortions

Sometimes, the necessity of reproducing exactly some typical geometries, as in the case of the human circulatory system, instead of using rectangular cross-section micro channels it is common to use circular cross-section micro channels. In this latter case, an special attention should be considered for matching the refractive index of the working fluid and of the channel in order to diminish optical distortions, hidden black regions and reflections that would affect the measurements of the experimental techniques. An schematic representation of the differences between a geometry with solid-liquid interfaces with curvature and without curvature is presented in Fig. 3.10, where a clear deviation of the rays is observed in the case of the circular geometry.

The real effect can be observed in Fig. 3.11, a circular cross-section milichannel made of PDMS is filled with different fluids having different refractive indices. For a refractive index of 1.33, much lower than that of PDMS, a wide black region close to the walls appears leading to a confusing detection of particle positions. If we increase the refractive index, close to that of the PDMS (1.41) [3], the distortion diminishes, allowing the correct characterization of the fluid-flow.

In the case of micro channels with a circular cross-section geometry the refractive index of the working fluid should match the refractive index of the micro channel material in order to avoid optical distortions.

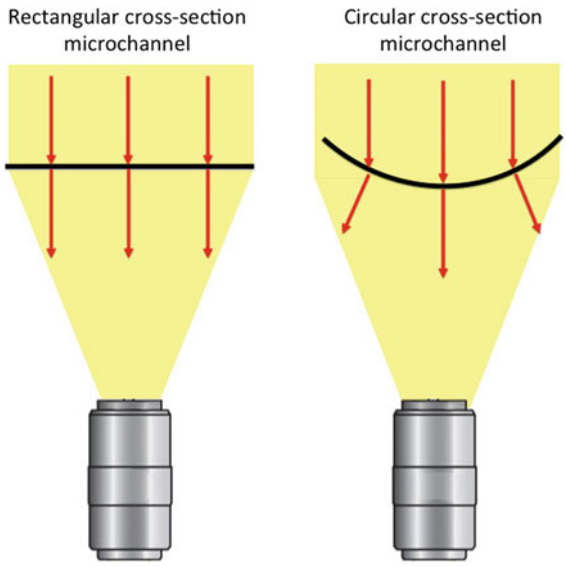

Fig. 3.10 Schematic representation of the refraction of light in a rectangular cross-section and in a circular cross-section micro channel

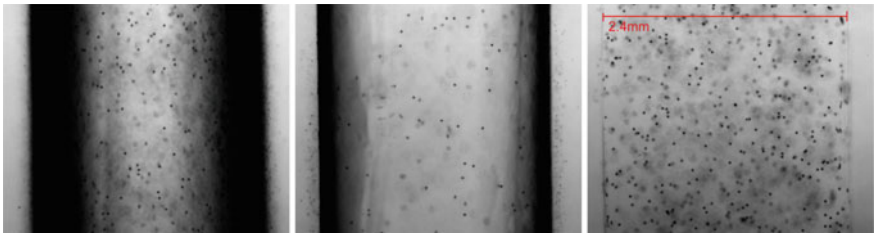

Fig. 3.11 Microscope images in the *middle plane* of a PDMS milli-channel with circular cross-section filled with solutions with different refractive index: 1.33 (*left*), 1.39 (*middle*), and 1.41 (*right*) containing 15.47 μm spherical particles (refractive index of PDMS was 1.41). Reproduced from [3], with the permission of AIP Publishing

3.3.2 Entrance Length and Exit Effects

When the working fluid is Newtonian the calculation of the entrance length (L_e) dimension is trivial, either in laminar or turbulent flows, although this latter case is not usual in microfluidics. However, when the fluid flow is non-Newtonian the characterization of the point at which the flow becomes totally developed is not an easy task. Elastic effects play a very important role and the determination of their influence in the entrance length is not well stablish until data. Only evaluating the velocity profile at different points along the micro channel will help to define this important length.

Li and Haward [31] investigated the flow of a Newtonian fluid and a viscoelastic fluid through a micro fabricated capillary entrance device. The concluded that the effect of the elasticity significantly increases the entrance length and it depends on the Wi number.

> The determination of the entrance length when the working fluid is non-Newtonian is not trivial. This distance could be only determined by measuring the velocity profiles along the micro channel.

The end effects are also very important and, as in the case of the entrance length, the distance between the exit and the area of interest must be long enough to avoid instabilities. The experimental determination of the velocity profile along the channel is the most accurate way to delimit this length.

The entrance and exit effects are particular important when the pressure drop need to be determined. There is an excess of pressure drop that can be corrected using the well-known Bagley correction [1].

3.3.3 Presence of Bubbles in Tubes and Channels

When the flow is injected into the micro channel through the syringe and the supply tubes, it is very common to notice the rise of some air bubbles. The presence of these bubbles affects the accuracy and reliability of the measurements. In order to solve this problem several options can be considered:

- In a first step the micro channels should be washed with ethanol and deionized water, after that the working fluid should be introduced [19].
- Increase the flow rate and keep the flow during long time. In the case of micro channels made of PDMS, as this material is porous it would help in the elimination of the air bubbles.
- Fill in completely the tubes with the fluid before connecting the syringe to the tube, the same with the syringe. In this way, no bubbles would enter in the instant of the connection.

The rising of air bubbles affects the flow and avoids the obtention of accurate and reliable measurements. It is important to verify that the micro channel is free of air bubbles.

3.3.4 Sedimentation of Particles

In the case of suspension in which the particles of the solution act as tracer particles, i.e. the study of flow behavior of cells in a viscoelastic medium, it is important to avoid the sedimentation of the particles. The sedimentation could appear either in the supply tubes or in the microchanel. In micro channels, taking into account the flow transient times this effect could be negligible being only important at very low flow rates. However, the sedimentation in the supply tubes and in the syringe could be more significant due to the long time the working fluid is inside the syringe during the experiment. Matching the density of the particle with the density of the solvent fluid is essential to reduce this problem.

The sedimentation is enhanced if the particles tend to form agglomerates. The addition of a surfactant, as Sodium Dodecyl Sulfate (SDS), in small amount around 0,05% helps to avoid the agglomeration. Dextran 40 is very commonly used in *in vitro* blood flow experimental studies as a substitute of blood plasma to diminish the sedimentation and clogging of the cells.

In the case of using fluorescence tracer particles, the proper selection of the size and concentration of these particles is crucial for accurate measurements. This aspect was already addressed in Sect. 3.2.2. However, other important phenomenon related to the adhesion of these particles in the micro channel walls must be also considered here. Figure 3.12 shows an example of an excess of light due to the concentration of

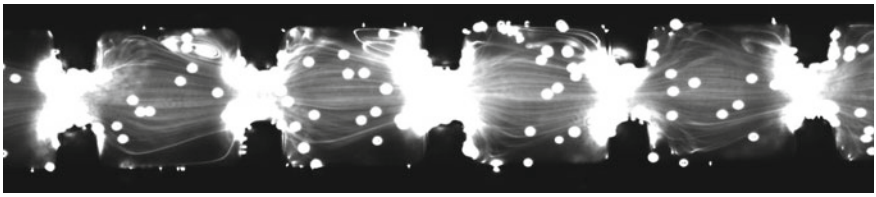

Fig. 3.12 Effect of the excited-state saturation of the tracer particles as a consequence of the stuck of the tracers in the channel walls

tracer particles in the walls of the micro channel. This excess of light is a consequence of excited-state saturation of the particles as they remain fixed to the walls during time. The addition of a surfactant will decrease considerably this undesirable effect. However, one should be careful with the addition of surfactant, as we may modify the rheological behaviour of our sample.

Sedimentation, aggregation and stuck of tracer particles in the channel or in the supply tubes should be avoided by adding specific solutions and by matching the density between particles and the working fluid.

3.3.5 Focusing the Mid Plane

One of the fundamental problems at the time to perform a microfluidic characterization technique, is the location of the mid plane. When the lens used is of low magnification, the problem is not important as the field of view of the lens is sometimes higher than the depth of the microchanel. However, when the magnification lens is high, it is crucial to find the focussing plane. In order to find the proper location of the focussing plane, the bottom part of the channel must be focused using the adjustment knob of the microscope (Fig. 3.13) trying to get the sharpest possible image, after that the lens is moved away in order to focus the top part of the micro channel and we proceed in the same way. The mid plane corresponds with the medium distance between these two focused walls.

Before performing any flow characterization technique, the focussing of the mid plane must be guaranteed.

Fig. 3.13 Knob of the microscope used for the adjustment of the focussed image

3.3.6 Pulses in Syringe Pumps

The pulses in the flow associated with the syringe pump when the flow rate is imposed are critical to reliable operation of microfluidic devices and could lead to undesired oscillations in the flow rate and pressure pulsations. The problem is caused by the mechanical operation of the pump. Basically, the problem occurs when the flow rate is very low or when the syringe size is not appropriate for the selected flow rate. In order to overcome this limitation, one should select thoroughly the volume of the syringe, a small syringe diameter improves the flow rate stability. It is important to take this into account when the expected stability is on the order of magnitude of 0,1 μL/min [9]. An alternative option is using a pressure pump that is free of pulses, as there is not any moving mechanical part connected to the fluid.

> The use of syringe pumps will introduce pulses that would lead to oscillations in the flow rate. The selection of the smaller syringe diameter according to each desirable flow rate is essential to overpass this limitation.

3.4 Remarks

Microfluidics techniques for the fluid-flow characterization have important applications. The selection and applicability of these techniques must be thoroughly examined in order to make the most of their potentialities. When the objective is just a qualitative assessment of the flow field, streak line photography is the most suitable method. However, when one needs to quantify the magnitude of the velocity field, the μ-PIV is the most recommendable technique. Nevertheless, the time comsuption

of the latter one is higher due to the data post processing, but with a more valuable information. Additionally, the μ-PIV is an expensive and bulky technique.

The characterization of the pressure drop in a micro device is also convenient even when the measurements are always the most complicated of all of the mentioned techniques. An excellent complement to all this information about the fluid flow is the determination of the stress distribution in polymer solutions that can be obtained using birefringence techniques.

3.5 Summary

In this book chapter the main microfluidic techniques used in the characterization of the complex fluid flows have been reviewed as well as some practical tips that may be help in their use.

#1 A proper design of the microfluidic set up is crucial for obtaining reliable and accurate measurements of the main flow characteristics.
#2 Knowing the potentialities and applicability of the available experimental techniques is crucial for the selection of the most appropriate method for fluid flow characterization.
#3 The applicability of FIB techniques requires the use of birefringent materials introducing a restriction to the fluids being used.
#4 Birefringence measurements provide the stress tensor directly only when the flow is considered to be 2D. Otherwise, for a 3D flow, the birefringence and the orientation angle vary along the light path leading to a cumulative measurement of the optical properties.
#5 In the case of micro channels with a circular cross-section geometry the refractive index of the working fluid should match the refractive index of the micro channel material in order to avoid optical distortions.
#6 The determination of the entrance length when the working fluid is non-Newtonian is not trivial. This distance could be only determined by measuring the velocity profiles along the micro channel.
#7 The rising of air bubbles affects the flow and avoids the obtention of accurate and reliable measurements. It is important to verify that the micro channel is free of air bubbles.
#8 Sedimentation, aggregation and stuck of tracer particles in the channel or in the supply tubes should be avoided by adding specific solutions and by matching the density between particles and the working fluid.
#9 Before performing any flow characterization technique, the focussing of the mid plane must be guaranteed.
#10 The use of syringe pumps will introduce pulses that would lead to oscillations in the flow rate. The selection of the smaller syringe diameter according to each desirable flow rate is essential to overpass this limitation.

References

1. Bagley, E. B. (1957). End corrections in the capillary flow of polyethylene. *Journal of Applied Physics*, *28*, 624–627.
2. Campo-Deaño, L., Galindo-Rosales, F. J., Oliveira, M. S. N., Alves, M. A., & Pinho, F. T. (2011). Flow of viscosity Boger fluids through a microfluidic hyperbolic contraction. *Journal of Non-Newtonian Fluid Mechanics*, *166*, 1286–1296.
3. Campo-Deaño, L., Dullens, R. P. A., Aarts, D. G. A. L., Pinho, F. T., & Oliveira, M. S. N. (2013). Viscoelasticity of blood and viscoelastic blood analogues for use in polydimethylsiloxane in vitro models of the circulatory system. *Biomicrofluidics*, *7*, 034102.
4. Campo-Deaño, L. (2016). Assessing the dynamic performance of microbots in complex fluid flows. *Applied Sciences*, *6*, 410.
5. Calejo, D., Pinho, D., Galindo-Rosales, F. J., Lima, R., & Campo-Deaño, L. (2016). Particulate blood analogues reproducing the erythrocytes cell free layer in a microfluidic device containing a hyperbolic contraction. *Micromachines*, *7*, 4.
6. Cheung, P., Toda-Peters, K., & Shen, A. Q. (2012). In situ pressure measurement within deformable rectangular polydimethylsiloxane microfluidic devices. *Biomicrofluidics*, *6*, 026501.
7. Durst, F., Melling, A., & Whitelaw, J. H. (1981). *Principles and practice of laser-Doppler anemometry* (2nd ed.). London: Academic Press.
8. Eaton, W. P., & Smith, J. H. (1997). Micromachined pressure sensors: review and recent developments. *Smart Materials and Structures*, *6*, 530–539.
9. Elveflow http://www.elveflow.com/microfluidic-tutorials/microfluidic-reviews-and-tutorials/syringe-pumps-and-microfluidics/stability-and-flow-oscillation-of-syringe-pumps-in-microfluidic/ Cited 30 April 2017.
10. Galindo-Rosales, F. J., Alves, M. A., & Oliveira, M. S. N. (2013). Microdevices for extensional rheometry of low viscosity elastic liquids: A review. *Microfluidics and Nanofluidics*, *14*, 1–19.
11. Galindo-Rosales, F. J., Oliveira, M. S. N., & Alves, M. A. (2014). Optimized cross-slot microdevice for homogeneous extension. *RSC Advances*, *4*, 7799–7804.
12. Haward, S. J., McKinley, G. H., & Shen, A. Q. (2016). Elastic instabilities in planar elongational flow of monodisperse polymer solutions. *Sicentific Reports*, *6*, 33029.
13. Larson, R. G., Khan, S. A., & Raju, V. R. (1988). Relaxation of Stress and Birefringence in Polymers of High Molecular Weight. *Journal of Rheology*, *32*, 145–161.
14. Martínez-Aranda, S., Galindo-Rosales, F. J., & Campo-Deaño, L. (2016). Complex flow dynamics around 3D microbot prototypes. *Soft Matter*, *12*, 2334–2347.
15. Mishra, S., Thakur, A., Redenti, S., & Vazquez, M. (2015). A model microfluidics-based system for the human and mouse retina. *Biomed Microdevices*, *17*, 107.
16. Mitsoulis, E. (1998). Numerical simulation of confined flow of polyethylene melts around a cylinder in a planar channel. *Journal of Non-Newtonian Fluid Mechanics*, *76*, 327–350.
17. Nam, S.-W., Choi, S., Cheong, Y., Kim, Y.-H., & Park, H.-K. (2015). Evaluation of aneurysm-associated wall shear stress related to morphological variations of circle of Willis using a microfluidic device. *Journal of Biomechanics*, *48*, 348–353.
18. Nguyen N.-T., Wereley, S. T. (2006). *Fundamental and applications of microfluidics*, (2nd ed.), Artech House, Boston.
19. Ober, T. J., Haward, S. J., Pipe, C. J., Soulages, J., & McKinley, G. H. (2013). Microfluidic extensional rheometry using a hyperbolic contraction geometry. *Rheologica Acta*, *52*, 529–546.
20. Oliveira, M. S. N., Alves, M. A., Pinho, F. T. (2011). Microfluidic flows of viscoelastic fluids. In R. Grigoriev (Ed.), *Transport and mixing in laminar flows: From microfluidics to oceanic currents*. Germany:Wiley-VCH Verlag GmbH & Co. KGaA, Weinheim.
21. Olsen, M. G., & Adrian, R. J. (2000). Out-of-focus effects on particle image visibility and correlation in microscopic particle image velocimetry. *Experiments in Fluids*, *29*, S166–S174.
22. Pan, L., & Arratia, P. E. (2013). A high-shear, low Reynolds number microfluidic rheometer. *Microfluidics and Nanofluidics*, *14*, 885–894.

23. Pipe, C. J., & McKinley, G. H. (2009). Microfluidic rheometry. *Mechanics Research Communications*, *36*, 110–120.
24. Pries, A. R., Secomb, T. W., Gaehtgens, P., & Gross, J. F. (1990). Blood flow in microvascular networks: Experiments and simulation. *Circulation Research*, *67*, 826–834.
25. Sinton, D. (2004). Microscale flow visualization. *Microfluidics and Nanofluidics*, *1*, 2–21.
26. Sousa, P. C. (2010). *Entry flow of viscoelastic fluids at macro- and micro- scale*. PhD Thesis.
27. Squires, T. M., & Quake, S. R. (2005). Microfluidics: Fluid physics at the nanoliter scale. *Reviews of Modern Physics*, *77*, 977.
28. Stone, S. W., Meinhart, C. D., & Wereley, S. T. (2002). A microfluidic-based nanoscope. *Experiments in Fluids*, *33*, 613–619.
29. Takahashi, T., & Fuller, G. (1996). Stress tensor measurement using birefringence in oblique transmission. *Rheologica Acta*, *35*, 297–302.
30. Wereley, S. T., & Meinhart, C. D. (2005). *Micron-resolution particle image velocimetry, in micro- and nanoscale diagnostic technologies*. New York: Springer-Verlag.
31. Haward, S. J., & Zhou, L. (2015). Viscoelastic flow development in planar microchannels. *Microfluidics and Nanofluidics*, *19*, 1123–1137.
32. Zijl, J. L. J. (2001). *Polymers in extensional flow. A comparison of microscopic and macroscopic simulations with birefringence experiments*. PhD Thesis.
33. Zilz, J., Schäfer, C., Wagner, C., Poole, R. J., Alves, M. A., & Lindner, A. (2014). Serpentine channels: micro-rheometers for fluid relaxation times. *Lab on a Chip*, *14*, 351.